

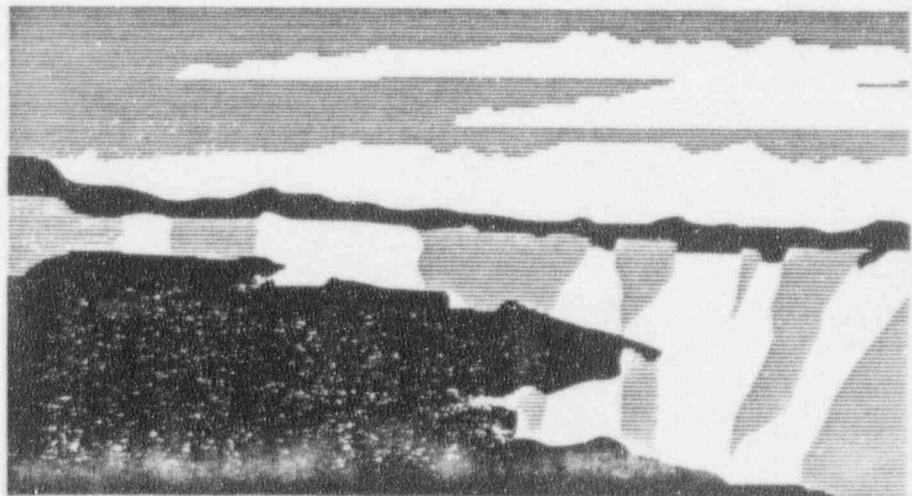
LA-UR-93-4282

Title: SMALL-BREAK LOSS-OF-COOLANT ACCIDENTS IN THE UPDATED
PIUS 600 ADVANCED REACTOR DESIGN

Author(s): B. E. Boyack, TSA-12
J. L. Steiner, TSA-12
S. C. Harmony, TSA-12
H. J. Stumpf, TSA-12
J. F. Lime, TSA-8

Submitted to: D. Ebert
Office of Nuclear Regulatory Research
USNRC

Los Alamos
NATIONAL LABORATORY



Los Alamos National Laboratory, an affirmative action/equal opportunity employer, is operated by the University of California for the U.S. Department of Energy under contract W-7405-ENG-36. By acceptance of this article, the publisher recognizes that the U.S. Government retains a nonexclusive, royalty-free license to publish or reproduce the published form of this contribution, or to allow others to do so, for U.S. Government purposes. The Los Alamos National Laboratory requests that the publisher identify this article as work performed under the auspices of the U.S. Department of Energy.

Form No. 836 R5
ST 2629 10/91

9402250113 940131
PDR PROJ
680

PDR

SMALL-BREAK LOSS-OF-COOLANT ACCIDENTS IN THE UPDATED PIUS 600 ADVANCED REACTOR DESIGN*

B. E. Boyack, J. L. Steiner, S. C. Harmony, H. J. Stumpf, and J. F. Lime
Technology and Safety Assessment Division
Los Alamos National Laboratory
Los Alamos, New Mexico 87545
(505) 667-2609

ABSTRACT

The PIUS advanced reactor is a 640-MWe pressurized water reactor developed by Asea Brown Boveri (ABB). A unique feature of the PIUS concept is the absence of mechanical control and shutdown rods. Reactivity is controlled by coolant boron concentration and the temperature of the moderator coolant. As part of the preapplication and eventual design certification process, advanced reactor applicants are required to submit neutronic and thermal-hydraulic safety analyses over a sufficient range of normal operation, transient conditions, and specified accident sequences. Los Alamos is supporting the US Nuclear Regulatory Commission's preapplication review of the PIUS reactor. A fully one-dimensional (1D) model of the PIUS reactor has been developed for the Transient Reactor Analysis Code, TRAC-PF1/MOD2. Early in 1992, ABB submitted a Supplemental Information Package describing recent design modifications. An important feature of the PIUS Supplement design was the addition of an active scram system that will function for most transient and accident conditions. Using TRAC and the 1D PIUS model, baseline calculations of the PIUS Supplement design were performed for small-break loss-of-coolant initiators at several locations in the PIUS reactor. In addition, sensitivity studies were performed to explore the robustness of the PIUS concept to severe off-normal conditions following a small-break loss-of-coolant accident. The sensitivity studies have examined partial flow blockage and boron dilution events, and these studies provide insights into the robustness of the design. TRAC-calculated results have been compared with 1D analyses prepared by ABB for the recently modified PIUS design.

INTRODUCTION

The PIUS advanced reactor is a four-loop, Asea Brown Boveri (ABB) designed pressurized water reactor with a nominal core rating of 2000 MWt and 640 MWe.¹ A primary design objective was to eliminate any possibility of a core degradation accident. A schematic of the basic PIUS reactor arrangement is shown in Fig. 1. Reactivity is controlled by coolant boron concentration and temperature, and there are no mechanical control or shutdown rods. The core is submerged in a large pool of highly borated water, and the core is in continuous communication with the pool water through pipe openings called density locks. The density locks provide a continuously open flow path between the primary system and the reactor pool. The reactor coolant pumps (RCPs) are operated so that there is a hydraulic balance in the density locks between the primary coolant loop and the pool, keeping the pool water and primary coolant separated during normal operation. Hot primary-system water is stably stratified over cold pool water in the density locks. PIUS contains an active scram system. The active scram system consists of four valved lines, one for each primary coolant loop, connecting the reactor pool to the inlets of the reactor coolant pumps. Although the active scram piping and valves are safety-class equipment, operation of the nonsafety-class reactor coolant pumps is required for effective delivery of pool water to the primary system. PIUS also has a passive scram system that functions should the active scram

*This work was funded by the US Nuclear Regulatory Commission's Office of Nuclear Regulatory Research.

system fail to operate for any reason. The passive scram system activates when the balance between the primary coolant loop and the pool is upset. Highly borated water from the pool enters the primary coolant via natural circulation from the pool, and coolant returns to the pool through the upper density lock. This process produces a reactor shutdown. The reactor pool can be cooled by either an active, nonsafety-class system or a fully passive, safety-class system.

As part of the preapplication and eventual design certification process, advanced reactor applicants are required to submit neutronic and thermal-hydraulic safety analyses over a sufficient range of normal operation, transient conditions, and specified accident sequences. ABB submitted a Preliminary Safety Information Document (PSID)² to the US Nuclear Regulatory Commission (NRC) for preapplication safety review in 1990. Early in 1992, ABB submitted a Supplemental Information Package to the NRC to reflect recent design modifications.³ The ABB safety analyses are based on results from the RIGEL code,⁴ a one-dimensional (1D) thermal-hydraulic system analysis code developed at ABB Atom for PIUS reactor analysis. An important feature of the PIUS Supplement design was the addition of the previously described active scram system that will function for most transient and accident conditions. However, this system cannot meet all scram requirements because the performance of the active scram system depends on the operation of the RCPs. Thus, the passive scram system of the original PSID design was retained. Because the PIUS reactor does not have the usual rod-based shutdown systems of existing and planned light water reactors, the behavior of the PIUS and shutdown phenomena following active and passive system scrams must be understood. Review and confirmation of the ABB safety analyses for the PIUS design constitute an important activity in the NRC's preapplication review. Los Alamos is supporting the NRC's preapplication review of the PIUS reactor. This paper summarizes the results of Transient Reactor Analysis Code (TRAC)⁵ baseline calculations for small-break loss-of-coolant accidents (SBLOCA) at several locations in the PIUS Supplement design. Sensitivity studies were performed to explore the robustness of the PIUS concept when exposed to severe off-normal conditions following a SBLOCA initiator. The sensitivity study results provide insights into the robustness of the design. Core neutronic performance was modeled with the TRAC point kinetics model.

TRAC ADEQUACY FOR THE PIUS APPLICATION

The TRAC-PF1/MOD2 code⁵ was used for each calculation. The TRAC code series was developed at Los Alamos to provide advanced, best-estimate predictions for postulated accidents in pressurized water reactors. The code incorporates four-component (liquid water, water vapor, liquid solute, and noncondensable gas), two-fluid (liquid and gas), and nonequilibrium modeling of thermal-hydraulic behavior. TRAC features flow-regime dependent constitutive equations, component modularity, multidimensional fluid dynamics, generalized heat structure modeling, and a complete control systems modeling capability. The code also features a three-dimensional, stability-enhancing, two-step method, which removes the Courant time-step limit within the vessel solution. Many of the features just identified have proved useful in modeling the PIUS reactor.

It is important that the issue of code adequacy for the PIUS application be addressed. If the TRAC analyses were supporting a design certification activity, a formal and structured code-adequacy demonstration would be desirable. One such approach would be to identify (1) representative PIUS transient and accidents sequences, (2) identify the key systems, components, processes and phenomena associated with the sequences, (3) conduct a bottom-up review of the individual TRAC models and correlations, and (4) conduct a top-down review of the total or integrated code performance relative to the needs assessed in steps 1 and 2. The bottom-up review determines the technical adequacy of each model by considering its pedigree, applicability, and fidelity to experimental separate effect or component data. The top-down review determines the technical adequacy of the integrated code by considering code applicability and fidelity to data taken in integral test facilities.

Because the NRC conducted a preapplication rather than a certification review, the NRC and Los Alamos concluded that a less extensive demonstration of code adequacy would suffice. Steps 1 and 2 were performed and documented in Ref. 6. A bottom-up review specific to the PIUS reactor was not conducted. However, the bottom-up review of TRAC conducted for another reactor type⁷ provided some confidence that many of the basic TRAC models and correlations are adequate, although some needed code modifications were also identified. A complete top-down review was not conducted. However, the ability of TRAC to model key PIUS systems, components, processes and phenomena was demonstrated in an assessment activity⁸ using integral data from the ATLE facility.⁴ ATLE is a 1/308 volume scale integral test facility that simulates the PIUS reactor. Key safety features and components were simulated in ATLE, including the upper and lower density locks, the reactor pool, pressurizer, core, riser, downcomer, reactor coolant pumps, and steam generators. Key processes were simulated in ATLE, including natural circulation through the upper and lower density locks, boron transport into the core (simulated with sodium sulfate), and control of the density lock interface. Core kinetics were indirectly simulated through a point kinetics computer model that calculated and controlled the core power based upon the core solute concentration and coolant temperature. All major trends and phenomena were correctly predicted. However, the calculated results were frequently outside the data uncertainty. None of the tests conducted in ATLE simulated severe transients such as loss-of-coolant accidents. Thus the assessment effort did not simulate some of the key processes and phenomena that are unique to loss-of-coolant accidents.

Benchmarking against another validated code is a second approach to demonstrating adequacy. In this paper, we will provide comparisons of TRAC- and RIGEL-calculated results for an identical SBLOCA initiator. These comparisons show reasonable qualitative and quantitative agreement in most, but not all, respects. The ability of TRAC to model key PIUS systems, components, processes and phenomena is supported, if not fully demonstrated, by benchmarking TRAC to the RIGEL code.⁴ The results of this SBLOCA benchmark comparison will be discussed at an appropriate point in this paper.

TRAC includes the capability for multidimensional modeling of the PIUS reactor. Indeed, multidimensional analyses of the passive scram via trip of one reactor coolant pump were completed for the original PSiD design.⁹ That study concluded that well-designed orificing of the pool water inlet pipes would minimize multidimensional effects. As a result of these earlier studies, we have concluded that 1D modeling has the potential for adequately representing many PIUS transients and accidents. We do note a reservation. The most important physical processes in PIUS are related to reactor shutdown because the PIUS reactor does not contain mechanical shutdown rods. Coupled core neutronic and thermal-hydraulic effects are possible, including multidimensional interactions arising from nonuniform introduction of boron across the core. ATLE does not simulate multidimensional effects. The RIGEL thermal-hydraulic model is 1D and a point kinetics model is used. Although both 1D and multidimensional TRAC thermal-hydraulic models have been used, core neutronics are simulated with a point kinetics model. At the present time, it is not known whether coupled core neutronic and thermal-hydraulic effects and multidimensional effects are important. We offer this important reservation along with the results that follow.

TRAC MODEL OF THE PIUS REACTOR

Figures 2 and 3 display the reactor vessel and coolant loop components of the TRAC 1D model. The 4-loop TRAC model consists of 74 hydrodynamic components (727 computational fluid cells) and 1 heat-structure component representing the fuel rods. The reactor power is calculated with a space-independent point-kinetics model. The hydrodynamic model has 8 components in each coolant loop and 16 components for the reactor vessel, with the remaining 26

components representing the pool, steam dome, density locks, and pressurizer line. The TRAC 1D model is more finely noded than the RIGEL model because of Los Alamos' modeling preferences, but no particular merit is attributed to the finer noding.

The TRAC steady-state and transient calculations were performed with TRAC-PF1/MOD2,⁵ version 5.3.05. The TRAC-calculated and PSID Supplement steady-state values are tabulated below for comparison.

	<u>TRAC</u>	<u>PSID Supplement</u>
Core mass flow (kg/s)	12822	12880
Core bypass flow (kg/s)	200.2	200
Loop flow (kg/s)	3255	3266
Cold-leg temperature (K)	531.0	527.1
Hot-leg temperature (K)	560.7	557.3
Pressurizer pressure (MPa)	9.5	9.5
Steam exit pressure (MPa)	4.0	4.0
Steam exit temperature (K)	540.3	543
Steam flow superheat (°C)	15.3	20
Steam and feedwater mass flow (kg/s)	243	243

Additional initial conditions for the calculated transients are as follows, except where otherwise noted for the sensitivity studies. The reactor is operating at beginning of cycle (BOC) with a primary loop boron concentration of 375 parts per million (ppm) and 100% power. The boron concentration in the reactor pool is initially 2200 ppm. If the active scram system is activated, the scram valves open over a period of 2 s following event initiation, remain open for 180 s, and close over a period of 30 s. The feedwater pumps are tripped as the scram is initiated and the feedwater flow rate decreases linearly to zero in 20 s. The steam pressure on the steam generator secondary side is kept constant at 3.88 MPa (steam drum).

PRESSURE RELIEF LINE SBLOCA

The initiating event for the baseline transient is a break in the pressure relief line at the flange just outside the steel pressure vessel and upstream of the safety relief valves. Steam flows through the break at a peak rate of 105 kg/s (Fig. 4, Frame 33) and then decreases with the primary pressure (Fig. 5, Frame 2). The mass flow through the break increases when two-phase flows begin to pass through the break. The two-phase flow develops after the primary system primary pressure falls below the secondary pressure, and steam in the steam generator secondaries condenses and adds energy to the primary. When the primary system depressurizes to 8.5 MPa at 18 s, a scram is initiated. The feedwater pumps are tripped and flows to the steam generators are terminated 20 s later. The scram valves operate as previously described. Injection of highly borated water into the primary system through the scram lines causes a rapid decrease in the core power to decay levels (Fig. 6, Frame 3). During the interval the scram valves are open, inventory is displaced from the primary system, through the upper and lower density locks, and into the reactor pool, as shown in Fig. 7 (Frame 7). However, closure of the scram valves induces a marked change in primary system behavior. While the scram valves are open, the flow of pool water to the inlet of each RCP varies between 200 and 150 kg/s and the REP inlets are full of liquid. Immediately following termination of the scram line flow, voiding occurs in the pump inlets (Fig. 8, Frame 30), the RCPs increase to their overspeed limit of 115% of nominal, and subsequently the pump discharges become oscillatory, as shown in Fig. 9 (Frame 14). The

oscillatory behavior propagates throughout the primary system. For example, the density lock flows oscillate, as shown in Fig. 7 (Frame 7). However, a net circulation pattern is established with pool water entering the primary system through the lower density lock and exiting the primary system through the upper density lock, as shown in Fig. 10 (Frame 20). The net inflow through the lower density lock produces a continuing, albeit oscillatory, increase in the primary boron concentration (Fig. 11, Frame 11). Coolant temperatures decrease, for the most part, throughout the transient (Fig. 12, Frame 12). However, the core inlet temperature increases following closure of the scram lines, and the core outlet periodically saturates as the core flow oscillates in concert with the RCP discharges.

We completed several sensitivity studies for the pressure relief line SBLOCA. The first sensitivity study examined the response of the PIUS reactor to the baseline SBLOCA concurrent with a 75% blockage of the lower density lock. The baseline and 75% blockage results were similar in all major trends and average quantities. There was, however, an important phenomenological difference between the two calculations. The baseline calculation displayed a strong oscillatory character when the RCP inlets voided following termination of the scram-line flows. The blockage case was markedly different. Oscillations, during the few intervals they existed, were much smaller and decayed with time. Density lock flows from the 75% blockage calculation are presented in Fig. 13 (Frame 7). These may be compared with the same parameters for the baseline calculation (Fig. 7). We offer the following explanation as a possible cause for the different system behaviors. When exposed to large inlet void fractions, the RCPs are operating in an inherently less stable regime, one subject to surging, for example. The PIUS system has a natural frequency and related harmonics. The open pathways between the primary system and the reactor pool help to characterize this natural frequency. We believe that in the baseline calculation, either the natural frequency or a harmonic matched the RCP behavior under partially voided inlet conditions to produce the system-wide oscillation. In both the baseline and sensitivity calculations, the same void existed in the RCP inlets. We hypothesize that partial blockage of the lower density lock "stiffened" the coupled primary-pool system with the result that pump-induced oscillations did not grow to detectable levels and, when they did become detectable, damped the oscillations.

The second sensitivity study examined the response of PIUS reactor to the baseline SBLOCA transient concurrent with a reactor pool boron concentration of 1800 ppm. The PIUS reactor will be tripped if the pool boron concentration falls below this level. The transient response throughout this transient was very similar to the baseline SBLOCA transient with nominal pool boron concentration. The decrease in reactor power to decay heat levels was slightly slower than in the baseline but the reactor powers were essentially equal after 200 s. Because the core power in the sensitivity study was slightly higher during the first 200 s of the transient, the primary system temperatures were also slightly elevated. As a result, the net natural-circulation flow between the reactor pool and the primary system was higher at the same transient time. In summary, the lowered pool boron concentration was of no consequence as the only impact was to slightly lengthen the time to reduce primary system temperatures to a given level.

The third sensitivity study examined the response of the PIUS reactor to the baseline SBLOCA concurrent with a failure of the active scram system. The scram valves are not permitted to open during this transient. Similar end states were reached for the two calculations by 1200 s when the transient calculations were terminated. The course of the sensitivity study transient differed, however, in several respects. Lacking the rapid injection of boron from the active scram system, core power decreased more slowly than in the baseline. Consequently, the buoyancy of coolant in the riser increased as core inlet and outlet coolant temperatures increased and voiding occurred in the core. The RCPs rapidly increased speed to the 115% overspeed limit in an attempt to control the position of the lower density lock thermal interface and did control the interface for 60 s. During this interval, the lower density lock was inactive and no boron entered the core. The lower density lock activated shortly after the pump overspeed limit was reached and highly borated water entered the primary system from the reactor pool. The initial decline in core power was due

to the negative reactivity insertions from increasing moderator temperatures and voiding in contrast to the baseline where the only source of negative reactivity insertion was from boron entering the core (Fig. 14, Frame 6). Oscillatory behavior occurred in both the baseline and sensitivity calculations once the RCP inlets voided.

A RIGEL calculation of a SBLOCA in the pressure relief line was reported in Ref. 3. Several results from the RIGEL calculations have been co-plotted with the TRAC-calculated results for this transient. The RIGEL calculations were terminated at 300 s while the TRAC calculations were terminated at 1200 s. The TRAC and RIGEL results are generally in qualitative agreement until 230 s when the scram valves close. The calculated break flow and pressurizer steam dome pressure histories are compared in Figs. 4 and 5, respectively. The calculated core power and pump mass flow histories are compared in Figs. 6 and 9, respectively. The boron concentration and temperature histories in the core region are compared in Figs. 11 and 12, respectively. There are moderate differences in the parameter values but the same trends are predicted by the two codes. SBLOCA tests have not been conducted in the ATLE facility, thus, no guidance regarding the relative accuracy of the two calculations can be provided. There are important phenomenological differences between the two calculations after 230 s. However, we believe that these differences arise from the timing at which events occur and, when considered in the perspective of extended transient times (e.g., 1200 s), are not significant. However, this conclusion is speculative because the RIGEL transient calculation was terminated at an early time. The TRAC-calculated results show the RCP controller demands an increase in speed at 210 s, about 10 s after the scram valves begin to close; the 115% RCP overspeed limit is reached by 260 s. The flow oscillations predicted by TRAC arise approximately 40 s after the RCPs have reached their overspeed limit and are caused by voiding in the inlets to the RCPs subsequent to closure of the scram valves. The RIGEL-calculated results show the RCP controller demands an increase in speed at 255 s, and the 115% overspeed limit is reached shortly before 300 s. We would expect that oscillatory RCP flows would be predicted by RIGEL at times greater than 300 s. We do note that a RIGEL calculation was performed for the same break location for the original PSID design.² During that transient, voiding arose in the inlets to the operating RCPs at 40 s, the RCP overspeed limit of 105% was reached at 50 s, and the RCPs outlet flows were oscillatory after 75 s.

SCRAM-LINE SBLOCA

The initiating event for this transient is a break in the loop-3 scram line at a location near the RCP inlet. The scram-line diameter and associated break area are 0.19 m and 0.028 m², respectively. Coolant is lost from both the pool and pump ends of the break in contrast to the pressure relief line break in which primary coolant is lost through only one end. The primary relief line is also smaller (0.1 m diameter and 0.0079 m²). Thus, the scram-line SBLOCA is a more severe accident when measured by the amount of coolant lost from the system. The pool-side and pump-side break flows are shown in Fig. 15 (Frame 33). Both break flows rapidly decrease from the maximum levels reached immediately following the break initiation. The decreasing break flows are the result of a rapidly falling primary system pressure (Fig. 16, Frame 2) and voiding at the break inlets. The pool-side break inlet is fully voided by 40 s, returns once to a two-phase flow, and remains fully voided after 60 s. Rapid voiding at the pool-side break inlet occurs as the pool water level drops to the elevation of the scram line connection. The pool liquid level remains near this elevation while primary system draining supplies the pump-side of the break. The pool-side break flow is terminated at 410 s when the pool liquid level resumes its decrease after the primary loops have drained. Two-phase fluid also appears at the pump-side break inlet beginning at about 40 s. The two-phase flow continues until about 700 s, although there is little liquid in the break flow after approximately 410 s when the liquid level within the riser falls below the level of the hot-leg attachments to the riser (Fig. 17, Frame 32). Between 40 and 380 s, the primary liquid level fluctuates around the elevation of the hot-leg attachments to the riser because the competing

mechanisms of RCP demand and supply in a partially voided environment. At 1200 s, the end of the calculated transient, the break flows are negligible (Fig. 15, Frame 33), and the liquid levels in the pool and riser are no longer decreasing. The liquid level has stabilized about 9 m about the top of the upper density locks.

The primary pressure history clearly reflects break-flow phenomena. During the interval from 0 to 40 s, liquid passes out both sides of the break and the pressure rapidly decreases (Fig. 16, Frame 2). From 40 to about 400 s, a slower rate of pressure decrease is established while two-phase flows pass through both sides of the break. At about 400 s, the pool-side break flow terminates and the rate of pressure decrease slows further. At approximately 800 s, the rate again decreases as the pool-side break flow approaches zero.

The instantaneous and integrated density lock flows are shown in Figs. 18 and 19 (Frames 7 and 20), respectively. Immediately after the break opens, there is a small flow of heavily borated pool water into the primary through the lower density lock. However, the primary early source of boron is from the active scram system, which starts operation on a low primary pressure signal. The active scram system is effective for only a brief period because the flows through the intact scram lines rapidly decrease when the pool liquid level approaches the elevation of the scram nozzle connections to the pool at 40 s. The negative reactivity inserted with these brief inflows of boron through the lower density lock and scram lines rapidly reduces the reactor power to 1250 MWt (Fig. 20, Frame 3). However, the RCP speed control system responds to this upset, recovers control of the thermal interface in the lower density lock, and terminates both the pool flow and the introduction of additional boron to continue the reactor shutdown. The flows through the three intact scram lines are small because the pool liquid level has decreased to the level of the scram-line inlet nozzles. During this time, the core flow is decreasing because the break reduces the flow of coolant to the core. With the core flow decreasing and the power decrease stalled, a power-to-flow mismatch occurs, a portion of the core coolant reaches saturation temperatures (Fig. 21, Frame 12), and brief intervals of core voiding occur. The void inserts negative reactivity and causes a further reduction in reactor power to about 300 MWt by 55 s. At this time, the RCP speeds reach the overspeed limit of 115%, the lower density lock fully activates, and flow through the lower density lock continues until the end of the calculated transient. The resultant introduction of boron (Fig. 22, Frame 11) completes the reduction of reactor power to shutdown levels.

For much of the transient, the flows through the upper and lower density locks are highly agitated. However, the integrated density lock flows clearly show a net natural circulation flow from the pool into the primary through the lower density lock, and a return flow to the pool via the upper density lock is established (Fig. 19, Frame 20). Thus, by 1200 s, the loss of coolant at the ends of the scram-line break is negligible, the reactor power is at shutdown levels, the loops are voided, and a natural circulation flow through the density locks is fully established.

SUMMARY OF OBSERVATIONS

1. The active and passive scram systems successfully accommodate the baseline pressure relief line and scram-line SBLOCA transients. The active scram system effectively reduces core power to decay levels for the baseline pressure relief line SBLOCA event. The passive scram system effectively reduces core power to decay levels for transients in which the scram system is inoperable (e.g., the baseline scram-line SBLOCA after the pool water level declines below the scram-line takeoff point).
2. The PIUS core, as presently designed, is characterized by compensating shutdown mechanisms. When highly borated pool water enters the primary through the lower density locks under baseline conditions, the negative reactivity associated with the boron is the primary mechanism for decreasing core power to decay heat levels. However, void and

moderator temperature increases are also effective mechanisms for reducing core power should conditions arise in the core that activate these reactivity insertion mechanisms.

3. Our confidence in the baseline simulations is enhanced by the assessment activity performed using ATLE data. The ATLE processes and phenomena were correctly predicted by TRAC. However, the phenomena in the ATLE tests conducted to date are not fully representative of SBLOCA conditions as no test simulates a loss-of-coolant accident. Moreover, there are quantitative discrepancies between key TRAC-calculated parameter values and the ATLE data. We would like to better understand the reasons for these differences should the PIUS design certification effort resume. More effort is required to identify whether the reasons for the discrepancies lie in our knowledge of the facility, modeling decisions made in preparing the TRAC input model of ATLE, or deficiencies in the TRAC models and correlations.
4. Our confidence in the predicted outcomes of the baseline simulations is enhanced by the code benchmark comparisons that were performed for the pressure relief line SBLOCA. The RIGEL- and TRAC-calculated results display many areas of similarity and agreement. However, there are also differences in the details of the transients and accidents calculated by the two codes, and we would like to better understand the reasons for these differences. It is desirable that the reasons for these differences be explored if the PIUS reactor progresses to the design certification stage. We do not feel that the differences are of sufficient import to alter the summary observations presented herein.
5. Although the sensitivity calculations move beyond both the assessment activity using ATLE data and the code-to-code benchmark activity with RIGEL, the PIUS design appears to accommodate marked departures from the baseline transient and accident conditions, including very low probability combination events. The studies of low pool boron concentrations and high fraction blockages of the lower density lock are characteristic of low probability events, yet these events appear to be successfully accommodated. No phenomenological "cliffs" were encountered for the sensitivity studies conducted.
6. At the present time, it is not known whether coupled multidimensional core neutronic and thermal-hydraulic effects are important. We believe that it will be important to investigate such effects should the PIUS reactor progress to the design certification stage.

REFERENCES

1. T. J. Pederson, "PIUS-A New Generation of Power Plants," Second ASME/JSME International Conference on Nuclear Engineering, San Francisco (March 21-24, 1993).
2. ABB Atom, "PIUS Preliminary Safety Information Document" (December 1989).
3. C. B. Brinkman, "PIUS PSID Supplemental Material," ABB Combustion Engineering Power document LD-93-020, Enclosure I (February 12, 1993).
4. D. Babala, U. Bredolt, and J. Kemppainen, "A Study of the Dynamics of the SECURE Reactors: Comparison of Experiments and Computations," *Nuclear Engineering and Design*, **122**, pp. 387-399 (1990).
5. N. M. Schnurr et al., "TRAC-PF1/MOD2 Code Manual - Theory Manual," Los Alamos National Laboratory document LA-12031-M, Vol. 1, NUREG/CR-5673 (to be issued).
6. B. E. Boyack, "Assessment of the PIUS Physics and Thermal-Hydraulic Experimental Data Bases," Los Alamos National Laboratory document LA-UR-93-3564 (1993).
7. B. E. Boyack and J. S. Elson, "Assessment of TRAC-PF1/MOD3 Code Adequacy for NP-HWR Thermal-Hydraulic Analyses," Los Alamos National Laboratory New Production Reactor document LA-NPR-TN-010 (September 15, 1992).
8. H. J. Stumpf, "TRAC Calculations of a Pump-Trip Scram and Partial Loss of Heat Sink for the ATLE Test Facility," Los Alamos National Laboratory document LA-UR-93-4133 (to be published).
9. J. F. Lime, J. S. Elson, J. L. Steiner, H. J. Stumpf, and B. E. Boyack, "Multidimensional TRAC Calculations of a Pump-Trip Scram for the PIUS 600 Advanced Reactor Design," Los Alamos National Laboratory document LA-UR-93-1184 (1993). Also to be published in the Proceedings of the ASME Annual Meeting to be held November 28-December 3, 1993, New Orleans, Louisiana.

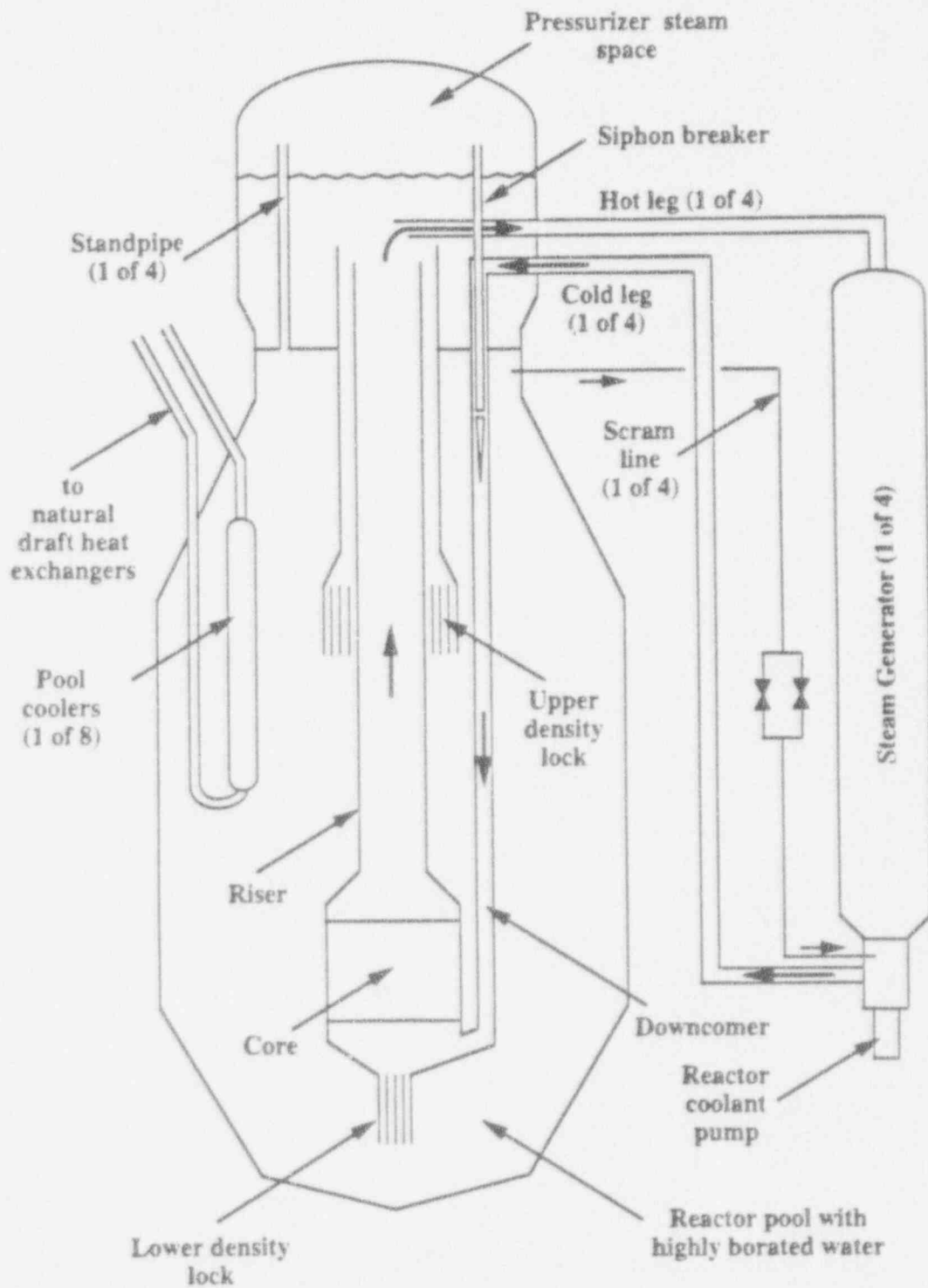


Fig. 1.
Schematic of the PIUS Reactor.

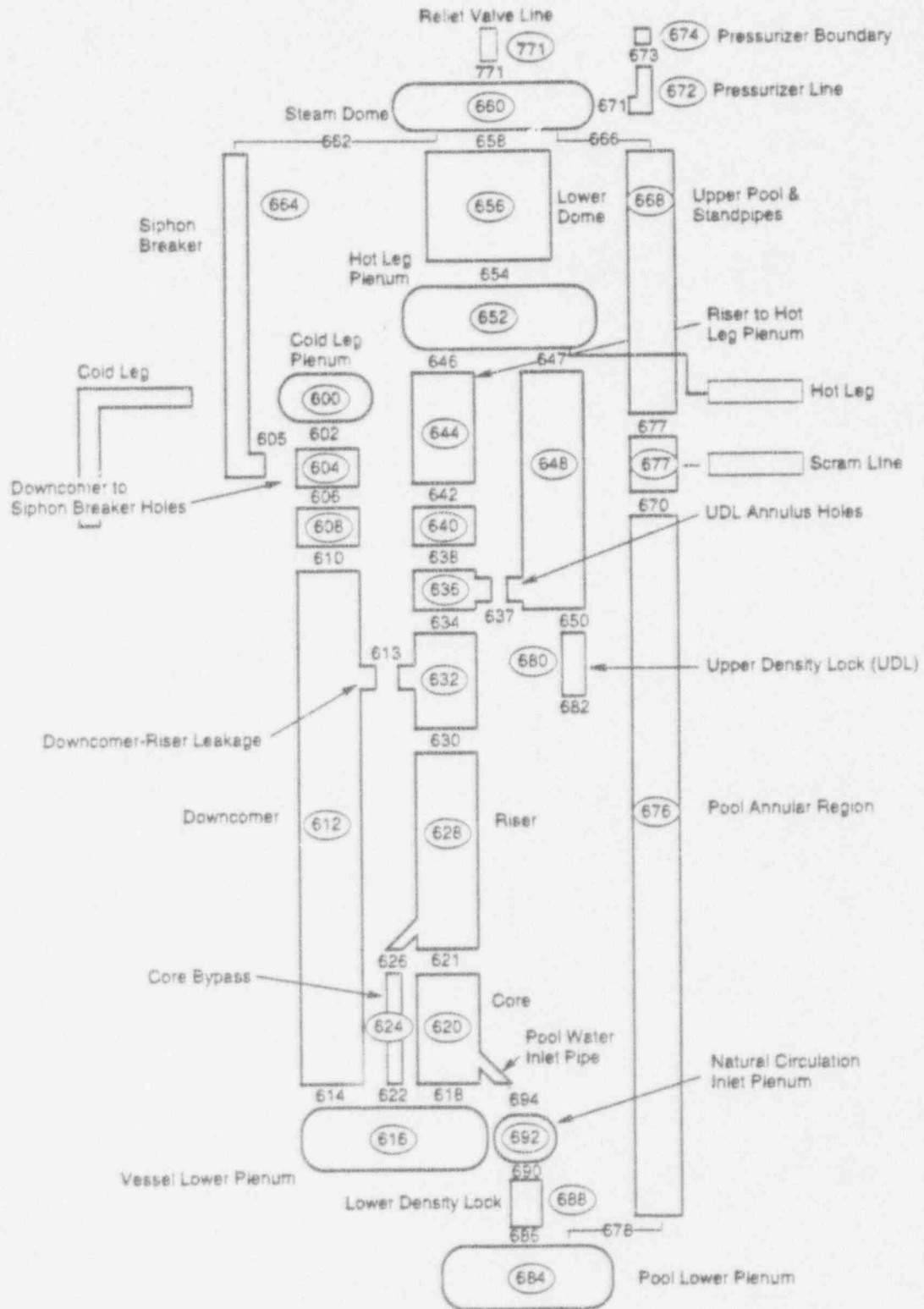


Fig. 2.
TRAC 1D model of the PIUS vessel and pool.

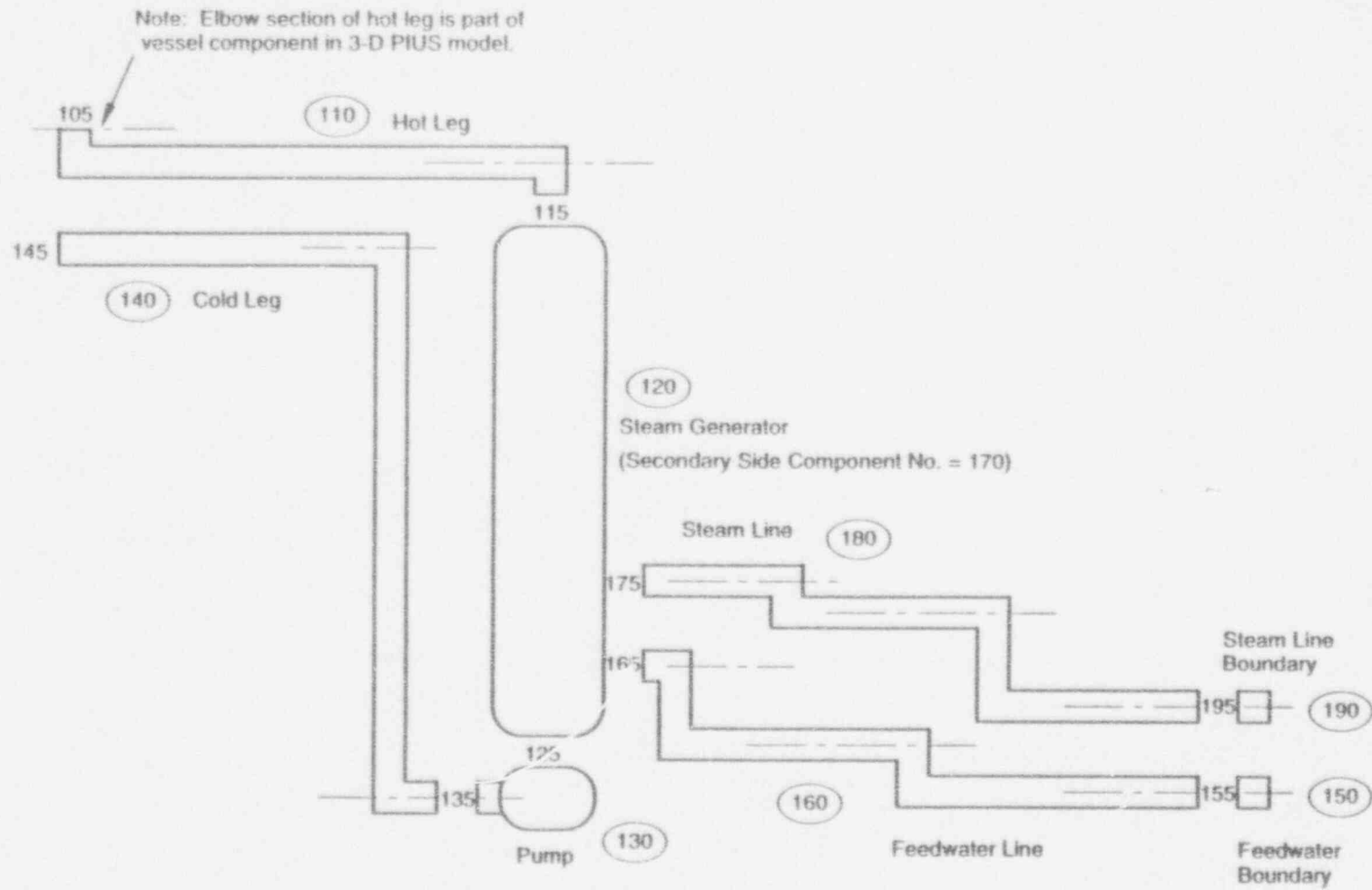


Fig. 3.
TRAC ID model of the PIUS coolant loops.

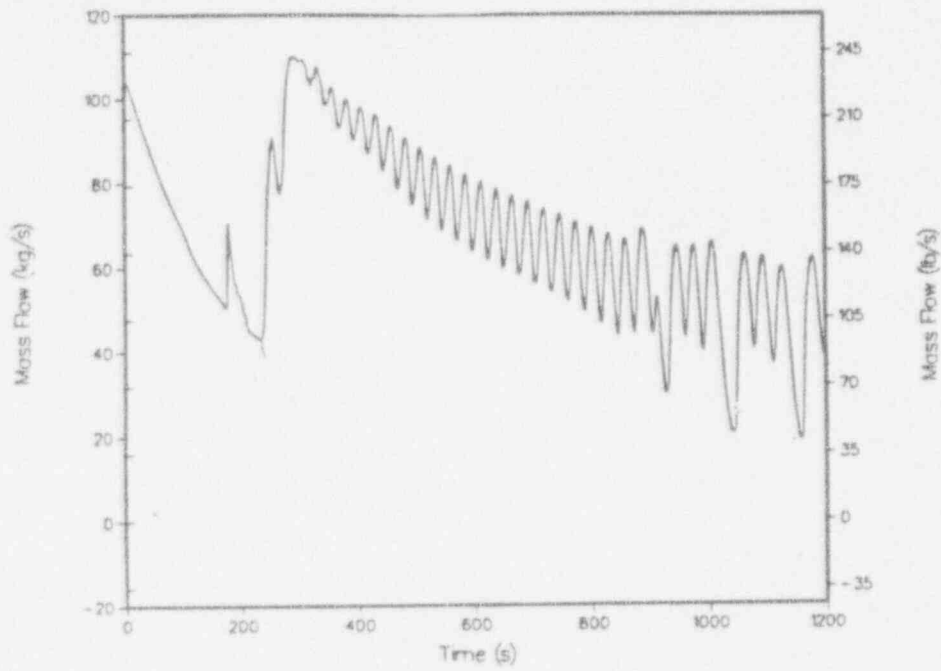


Fig. 4.
Break flows for pressure relief line SBLOCA baseline case.

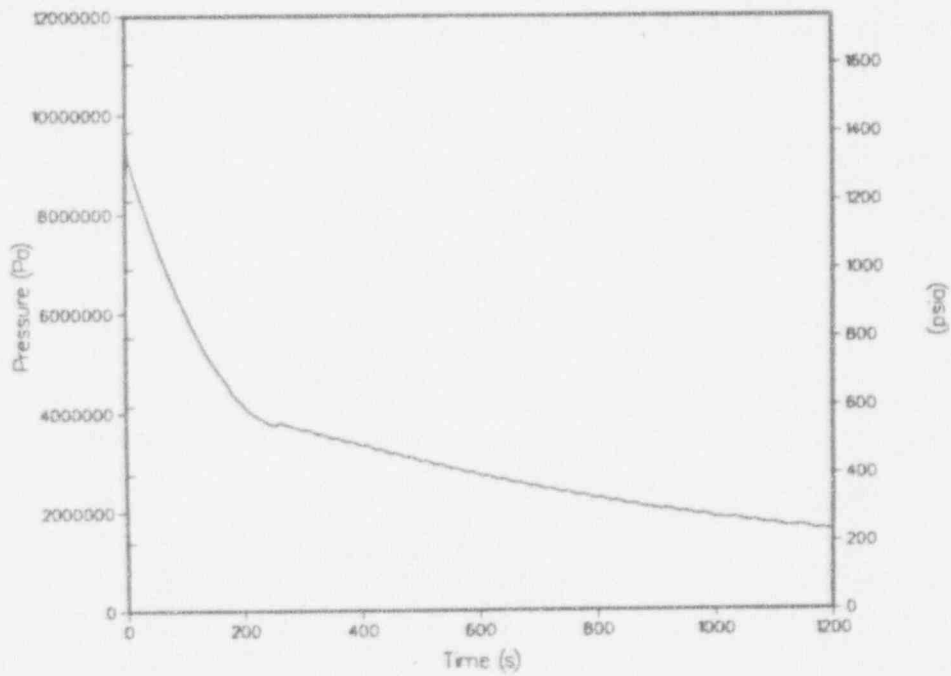


Fig. 5.
Pressurizer pressure for pressure relief line SBLOCA baseline case.

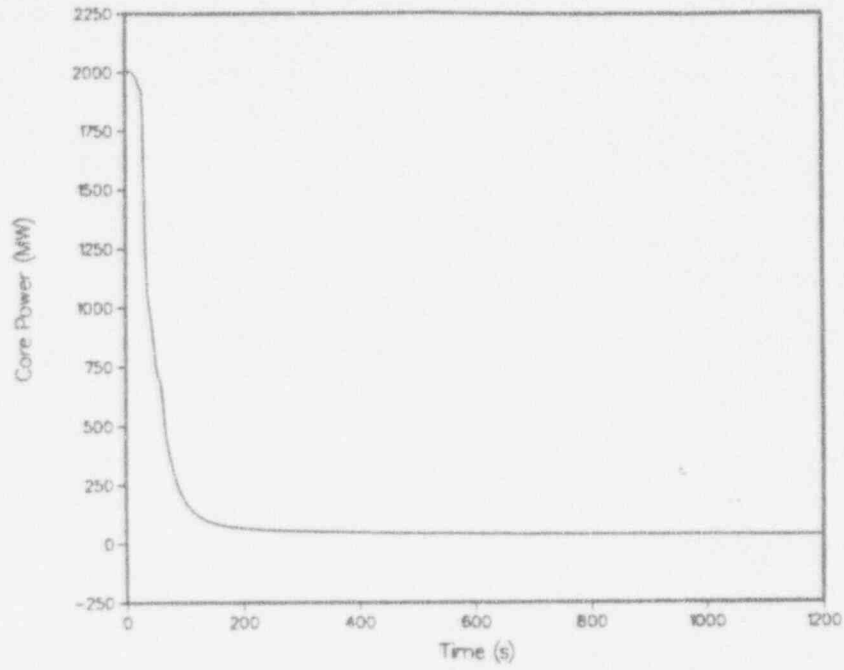


Fig. 6.
Reactor power for pressure relief line SBLOCA baseline case.

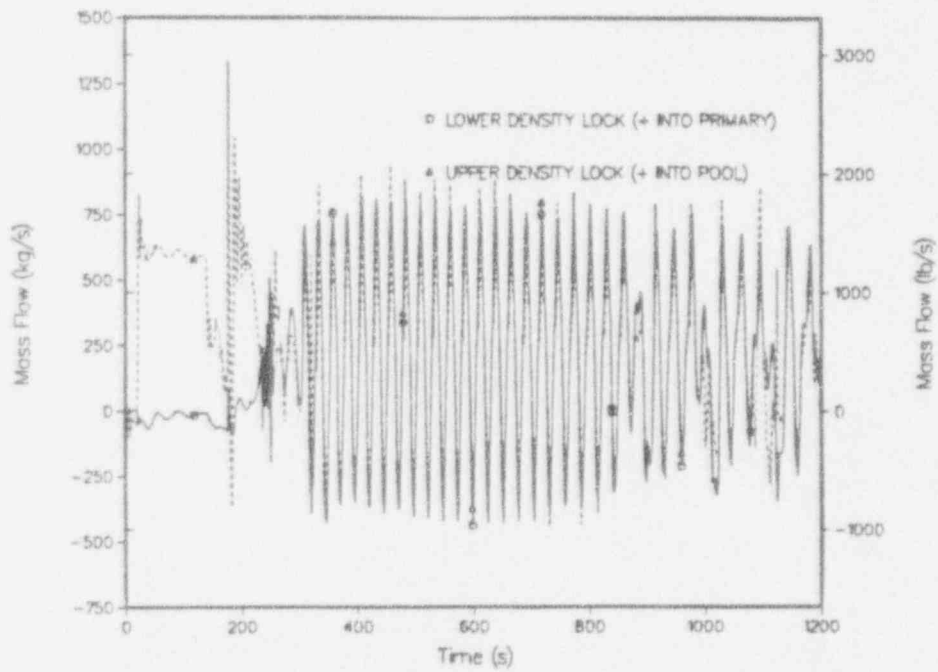


Fig. 7.
Density lock flows for pressure relief line SBLOCA baseline case.

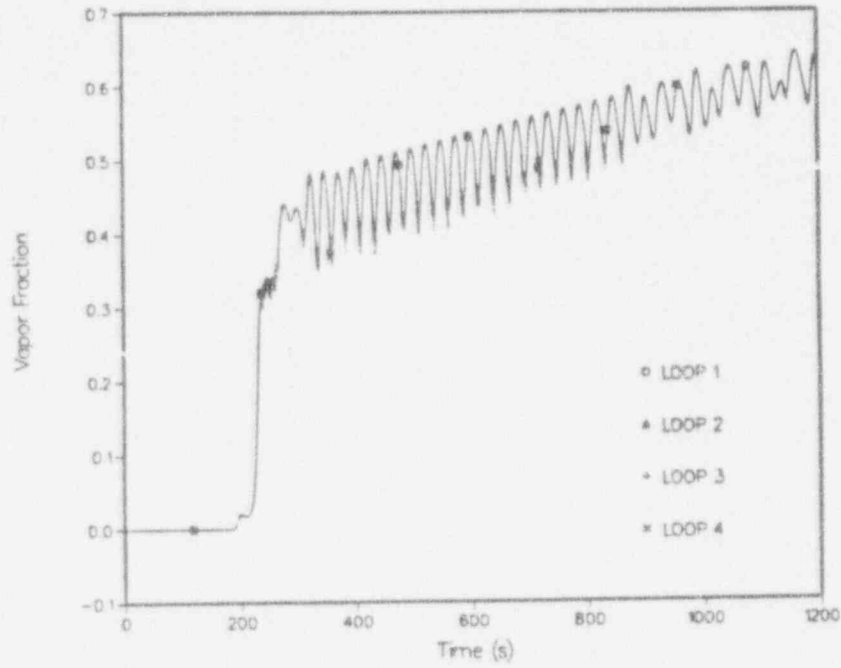


Fig. 8.
RCP inlet void fraction for pressure relief line SBLOCA baseline case.

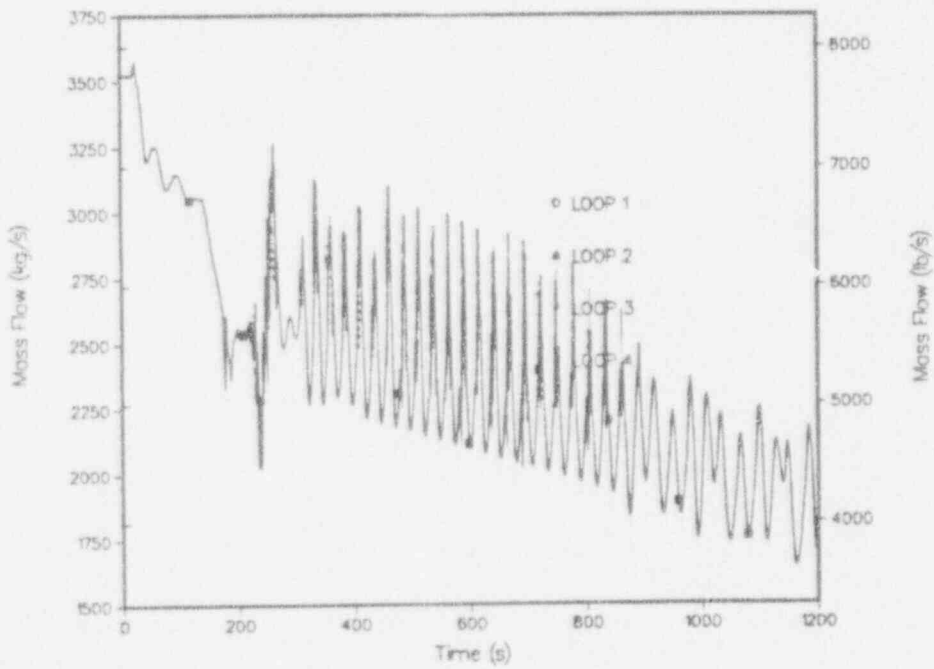


Fig. 9.
RCP outlet flows for pressure relief line SBLOCA baseline case.

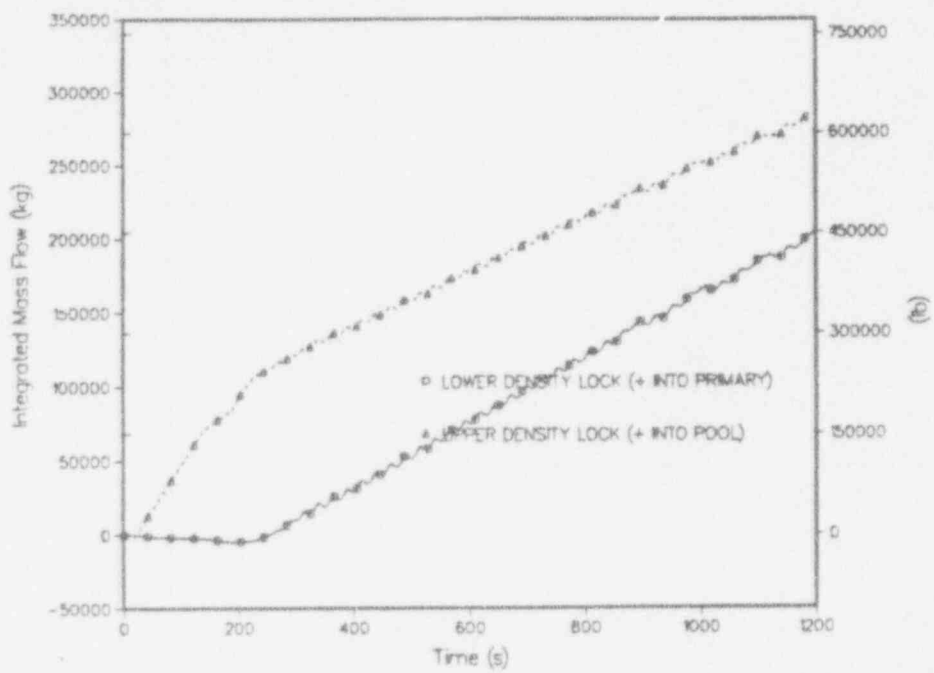


Fig. 10.
Integrated density lock flows for pressure relief line SBLOCA baseline case.

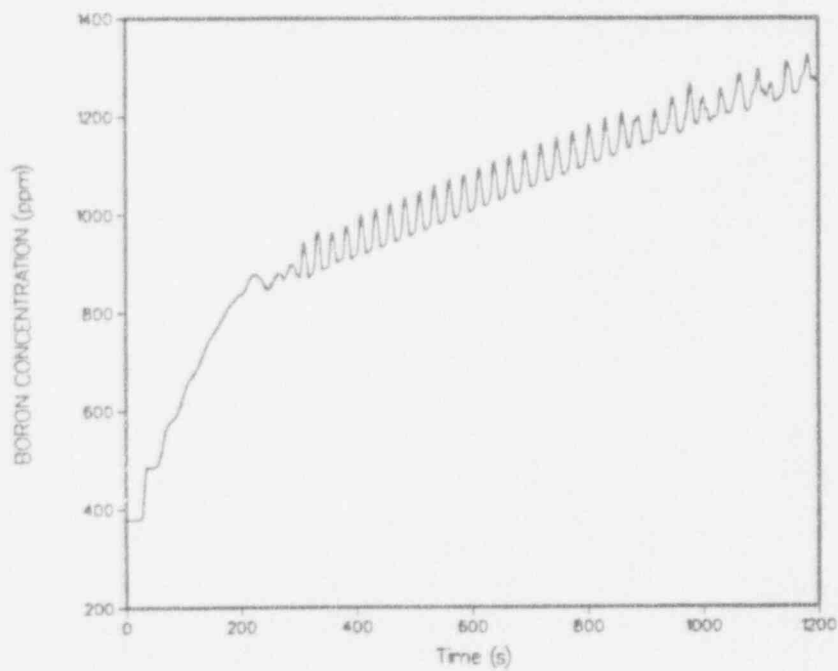


Fig. 11.
Primary boron concentration for pressure relief line SBLOCA baseline case.

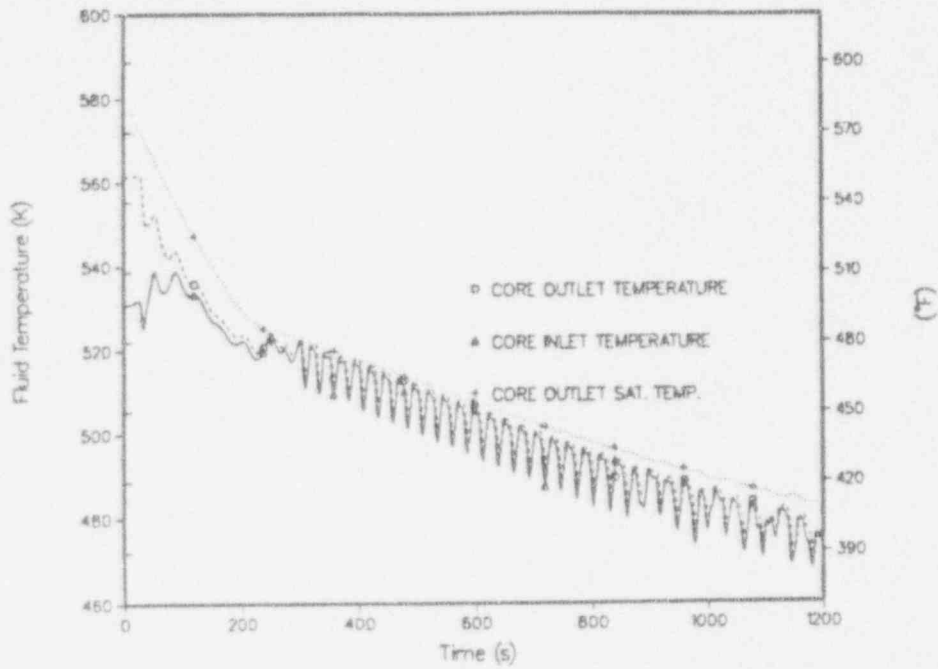


Fig. 12.
Core coolant temperatures for pressure relief line SBLOCA baseline case.

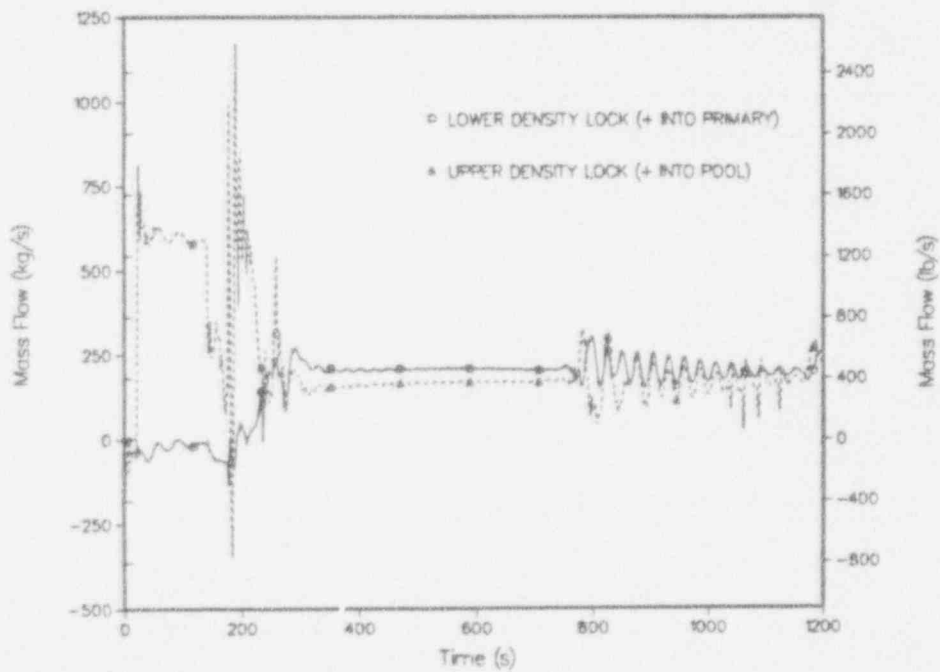


Fig. 13.
Density lock flows for pressure relief line SBLOCA with 75% blockage of the lower density lock.

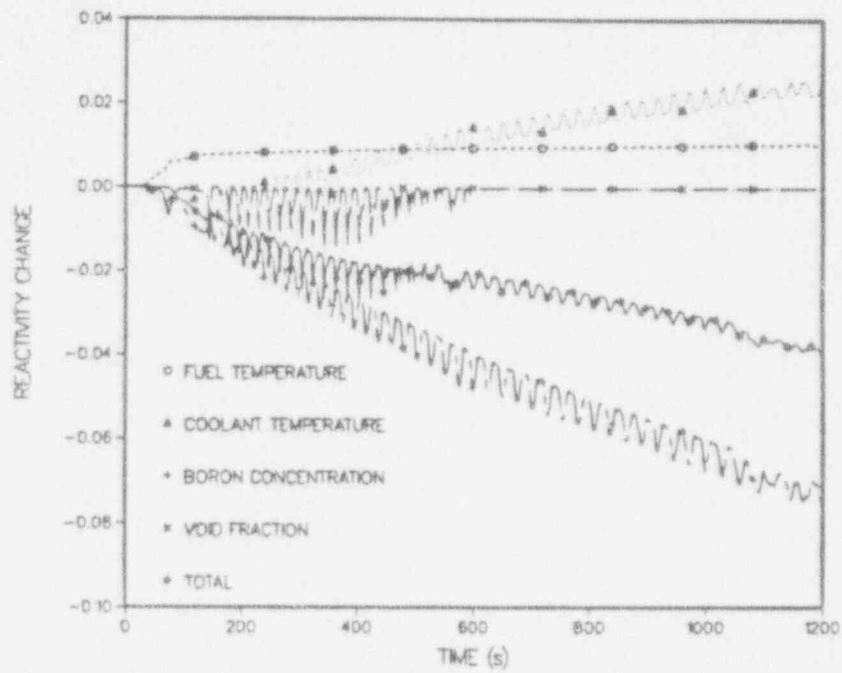


Fig. 14.
Core reactivity changes for pressure relief line SBLOCA with failure of the active scram system.

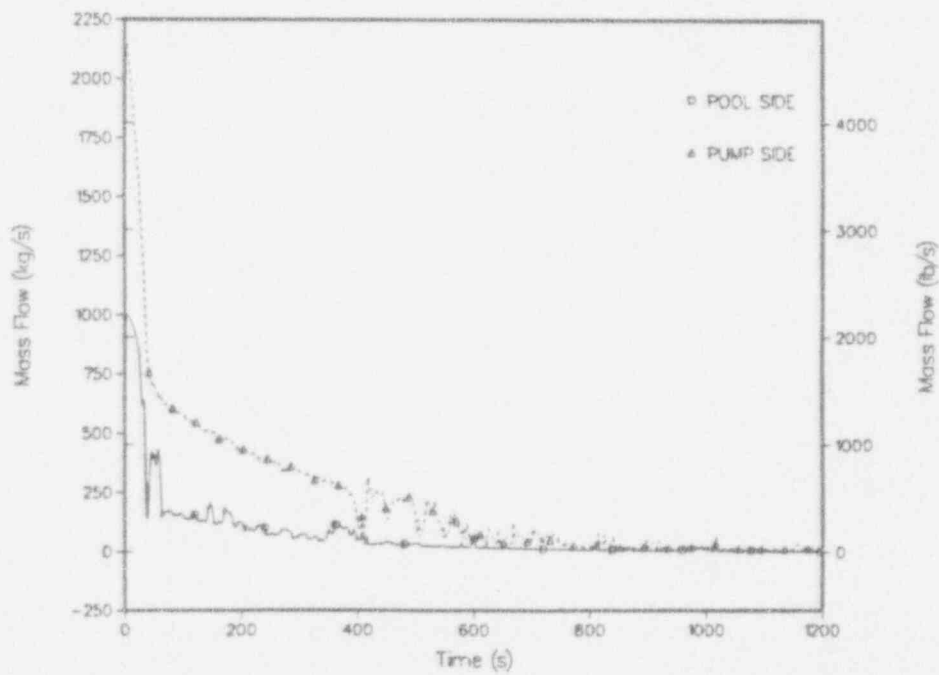


Fig. 15.
Break flows for a scram-line SBLOCA.

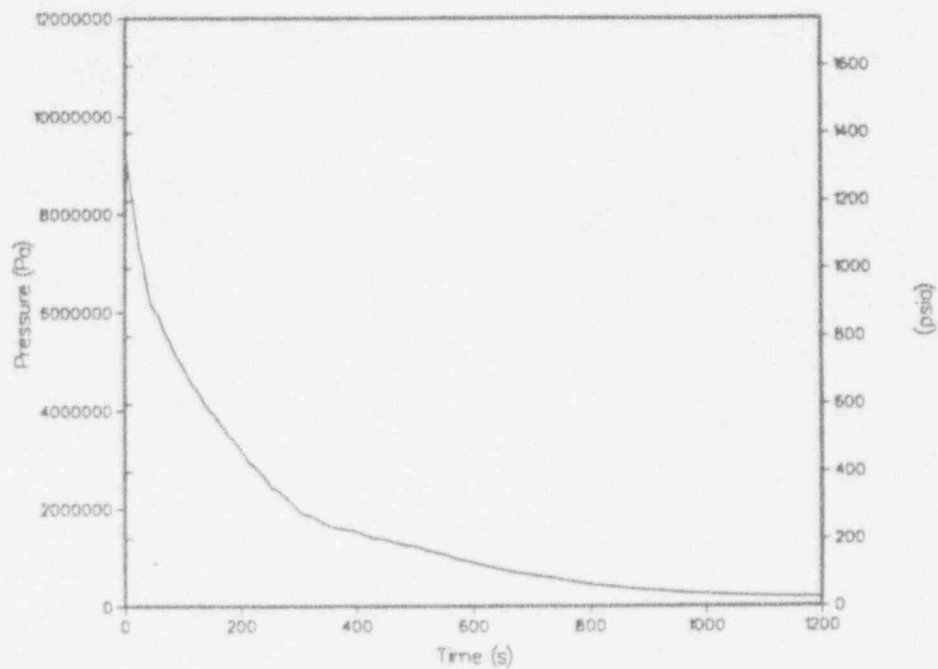


Fig. 16.
Pressurizer pressure for a scram-line SBLOCA.

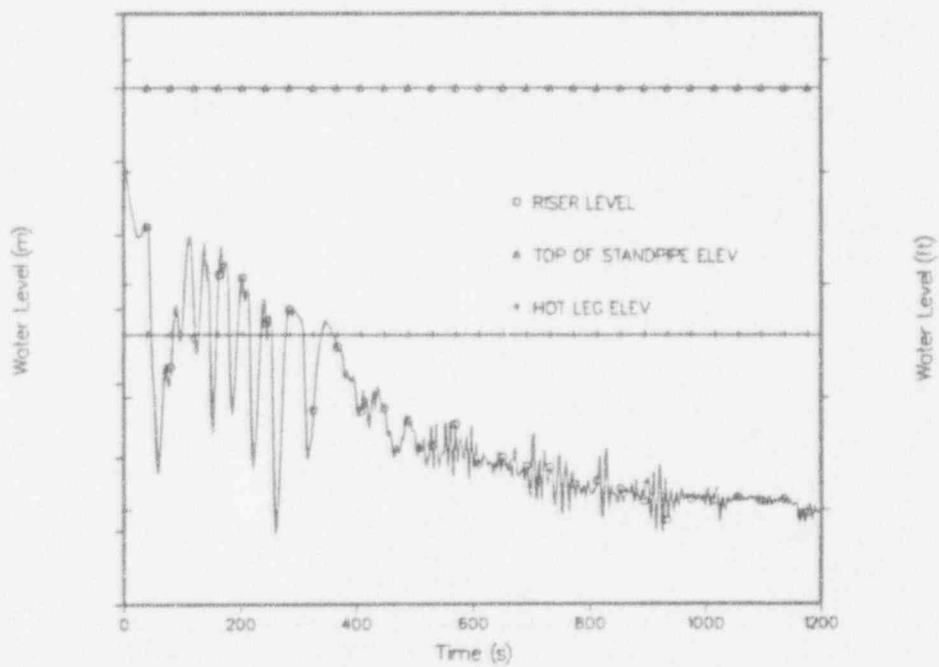


Fig. 17.
Riser collapsed liquid level for a scram-line SBLOCA.

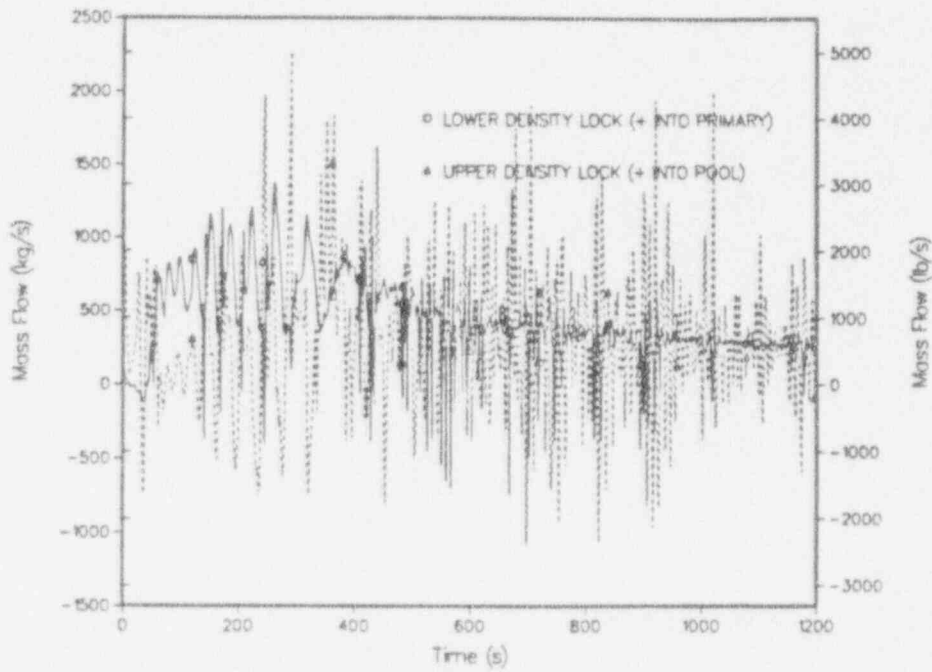


Fig. 18.
Density lock flows for a scram-line SBLOCA.

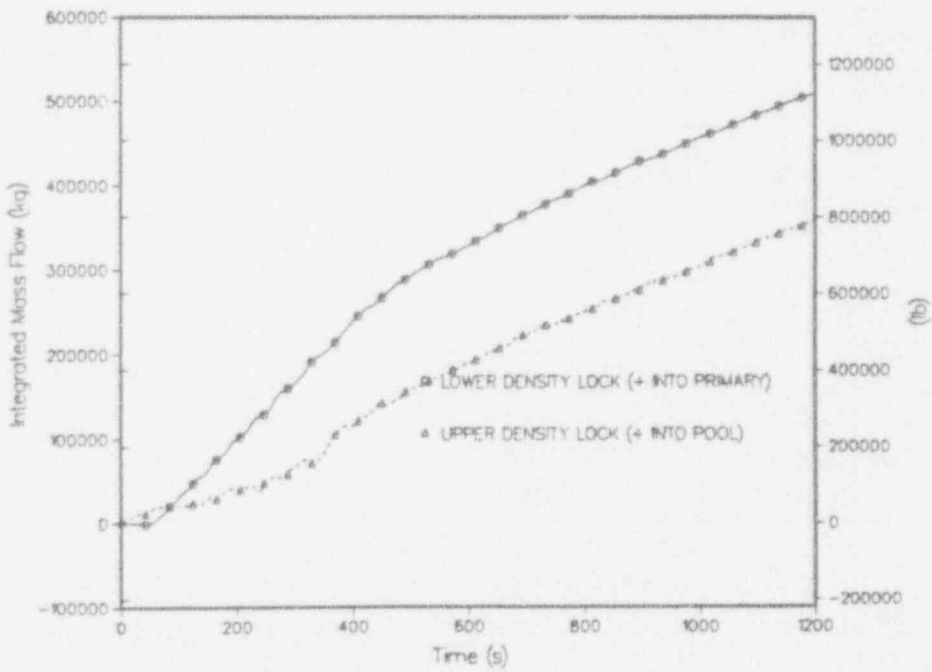


Fig. 19.
Integrated density lock flows for a scram-line SBLOCA.

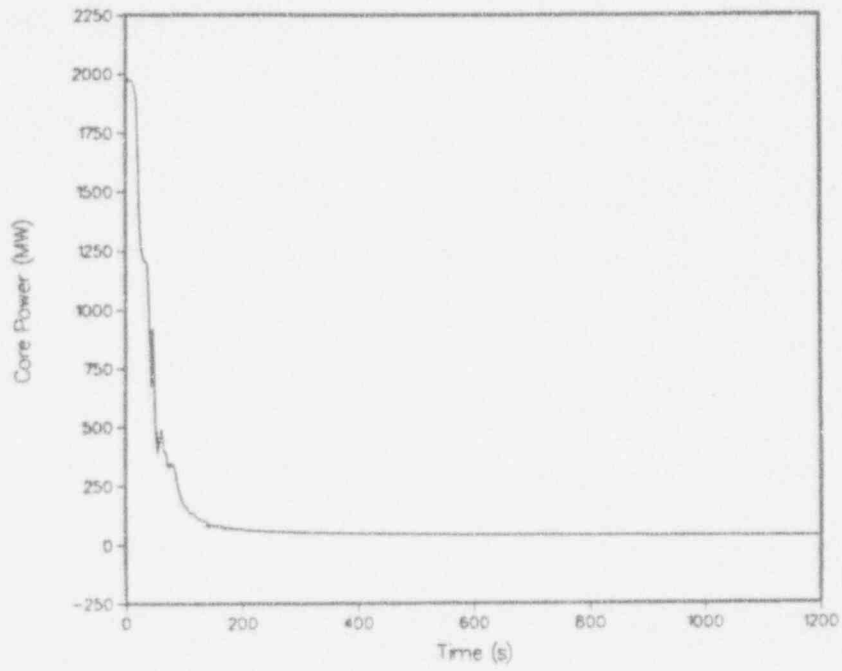


Fig. 20.
Reactor power for a scram-line SBLOCA.

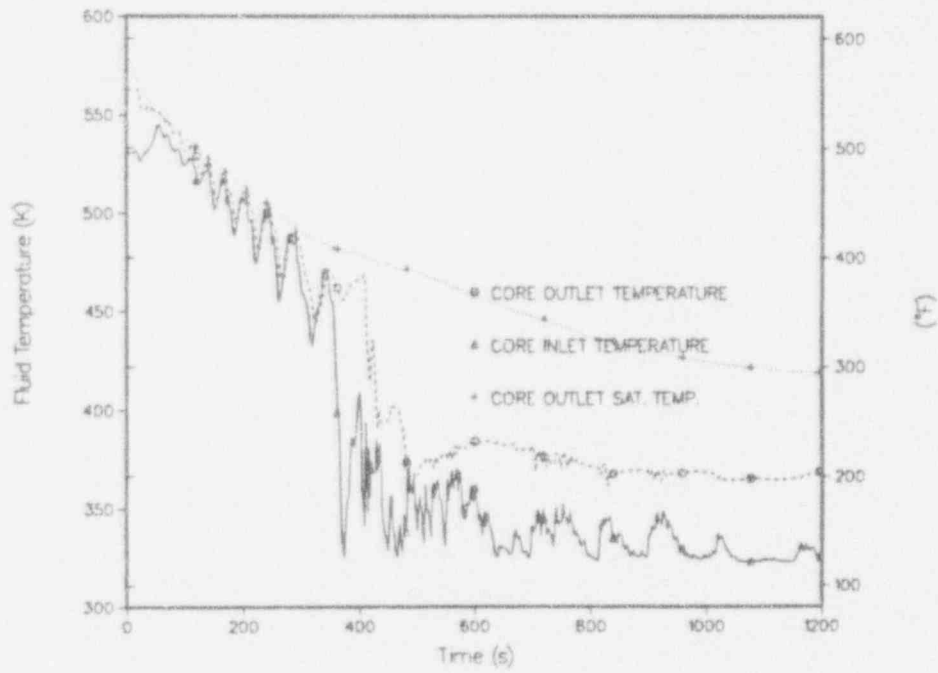


Fig. 21.
Core coolant temperatures for a scram-line SBLOCA.

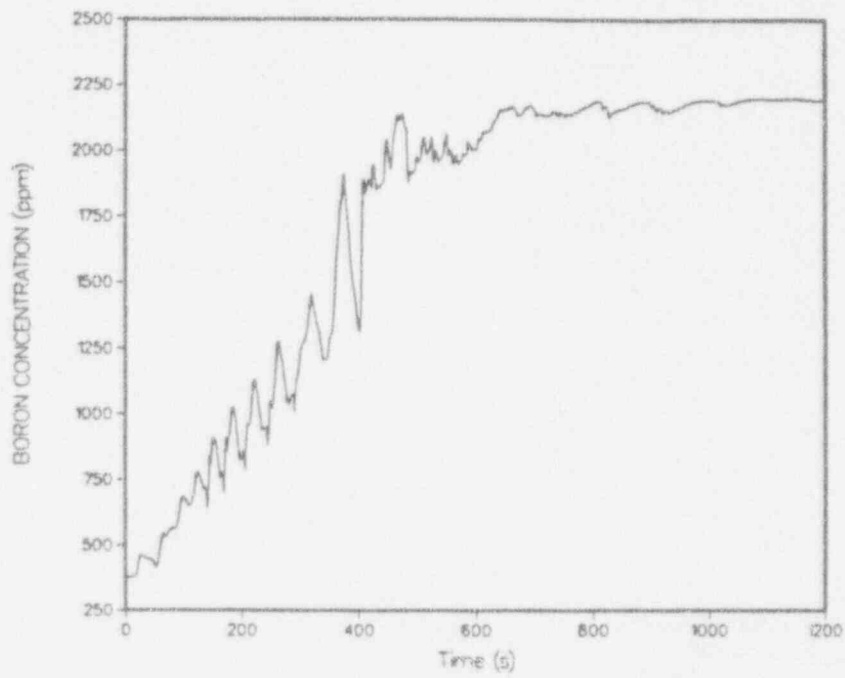


Fig. 22.
Core inlet boron concentration for a scram-line SBLOCA.